Effect of cooling rate on charge ordering in theta-(BEDT-TTF)(2)RbZn(SCN)(4)

F. Nad, Pierre Monceau, H.M. Yamamoto

Effect of cooling rate on charge ordering in θ-(BEDT-TTF)$_2$RbZn(SCN)$_4$

F. Nad
Institut Néel, CNRS-UJF, Bâtiment E, 25 rue des martyrs, Boîte Postale 166, 38042 Grenoble Cedex 9, France and Institut of Radioengineering and Electronics, RAS, Mokhovaya 11/7, 125009 Moscow, Russia

P. Monceau
Institut Néel, CNRS-UJF, Bâtiment E, 25 rue des Martyrs, BP 166, 38042 Grenoble Cedex 9, France

H. M. Yamamoto
Condensed Molecular Materials Laboratories RIKEN, 2-1 Hirosawa Wako-shi, Saitama 351-0198, Japan
(Received 18 April 2007; revised manuscript received 13 July 2007; published 5 November 2007)

We present results of measurements of the conductance and dielectric permittivity at various cooling and heating rates through the phase transition into the charge-ordered state in θ-(BEDT-TTF)$_2$RbZn(SCN)$_4$, [where BEDT-TTF is bis(ethylene-dithio)tetrathiafulvalene]. With increasing cooling rate, the sharpnesss of the first-order phase transition and the divergence of the dielectric permittivity associated with it are gradually suppressed. We explain the obtained results by the suggestion of combined contributions of electron and lattice subsystems to the formation of the charge-ordered state in two-dimensional organic compounds.

DOI: 10.1103/PhysRevB.76.205101 PACS number(s): 71.20.Rv, 71.30.+h, 77.22.Ch

I. INTRODUCTION

The effects of Coulomb interactions in low-dimensional organic conductors have recently raised great interest.[1] Strong correlations induce the formation of a superstructure which is driven by charge separation and localization at atomic sites. This spatially modulated charge, often called stripe order, has been observed in many strongly correlated systems, such as high-critical-temperature superconductors,[2] manganites,[3] and organic conductors. The possibility of charge ordering (CO) in two-dimensional (2D) organic conductors was suggested theoretically by Kino and Fukuyama[4] in (BEDT-TTF)$_2X$ salts [namely, in θ(BEDT-TTF)$_2$I$_3$], where BEDT-TTF is bis(ethylene-dithio)tetrathiafulvalene (alternatively abbreviated as ET) and X is a monovalent anion.

Another two-dimensional ET compound, θ-(BEDT-TTF)$_2$RbZn(SCN)$_4$, although it has a 3/4-filled conducting band and therefore should behave as a two-dimensional metal at room temperature, in the conditions of slow cooling undergoes a first-order phase transition around T_{CO}=200 K.[5,6] This transition is associated with the doubling of the unit cell along the c axis with a large displacement (about 0.2 Å) of ET molecules below T_{CO}.[6,7]

θ-(ET)$_2$RbZn(SCN)$_4$ is a layered material composed of conducting ET layers and insulating RbZn(SCN)$_4$ layers alternatively stacked along the b axis (interlayer direction). The packing pattern is such that the ET molecules in the conducting layer are disposed along a triangular lattice with one hole for every two molecules.

The real nature of the phase transition in θ-(ET)$_2$RbZn(SCN)$_4$ (below abbreviated as θ-RbZn) has only recently been determined[8–10] by NMR as being due to charge ordering. A drastic change in NMR line shape was found below T_{CO} with evidence of charge-rich and charge-poor sites. Raman spectroscopy on θ-RbZn has revealed a split of the charge-sensitive C=C stretching mode, indicating a charge difference among ET molecules at nonequivalent sites.[11] The charge distribution confirms the appearance of charge disproportionation (CD) below T_{CO} with an average CD ratio 0.2–0.8.

Moreover, it was shown that, in θ-RbZn, a specific CD already appears in the high-temperature phase well above T_{CO}.[12–14] This CD is associated with short-range slow charge fluctuations. The transition near 200 K might correspond to the formation of 3D long-range ordering assisted by a lattice dimerization along the c axis.

Studies of the roles of both on-site and intersite Coulomb interactions on the electronic states in (ET)$_2X$ compounds[15,16] predict stabilization of the charge-ordered states of stripe type. Different spatial charge patterns (horizontal, vertical, or diagonal) were proposed depending on the balance between anisotropic transfer integrals in the donor plane and the anisotropic intersite Coulomb interaction V.[15] The loss of the inversion center in the insulating phase of θ-RbZn, as concluded from the selection rule in Raman measurements, suggests that the charge is ordered along horizontal stripes. From structural data obtained at 90 K, the ionicities of the ET molecules in θ-RbZn were estimated from the intramolecular bond-length distribution; "charge-rich" and "charge-poor" sites were found with ionicities 0−+0.2 and 0.8−+1.0, with a spatial pattern consisting of 1D chains containing only hole-rich and hole-poor molecules alternating along the c axis.[7] This CO and its spatial pattern agree also with reflectance spectra and results from polarized Raman and infrared spectroscopy.[17,18]

The magnetic susceptibility χ does not show any anomaly at T_{CO}. The magnetic susceptibility slightly increases, with a maximum around 180 K, decreases gradually down to 25 K, then suddenly drops below 25 K and increases rapidly below 10 K.[19] The Curie contribution at low temperatures, less than 1%, is due to residual spins. After subtraction of the Curie spin magnetization, the T dependence of the magnetic susceptibility of θ-RbZn shows a Bonner-Fisher-like behavior characteristic of low-dimensional spin systems. The mag-

netic properties of this stripe-type CO state can be described by $S=1/2$ 1D Heisenberg models with magnetic interactions, the estimated exchange energy being $J=-157$ K between localized spins on the charge-rich sites along the charge stripes.[20] χ shows a magnetic transition below about 25 K to a (nonmagnetic) spin-gapped state due to the additional instability of the 1D Heisenberg chains of the localized spins along the stripes, i.e., a spin-Peierls transition.[21,22] χ can be fitted by a singlet-triplet model with $J=-45$ K.

χ depends strongly on the cooling rate around T_{CO}.[6,23,24] In fast cooling conditions, the magnetic susceptibility is the same as in slow cooling from 300 to 190 K. Below this temperature, χ increases continuously down to 2 K, showing enhancement of the Curie-tail contribution below 90 K without a sudden decrease below 40 K. The quenched (Q) state suppresses the spin-Peierls state. The ground state might be an antiferromagnetic state. So the lattice modulation does not occur in the rapid cooling and the singlet state is not obtained at low T.

Differences between the rapid-cooled state (Q state) and slow-cooled, relaxed state (R state) were also found in NMR, electron paramagnetic resonance EPR, and some transport properties.[22,25] Concerning the variation of resistivity near T_{CO} it was only mentioned that the first-order transition is replaced by a "gradual increase of resistivity" at a cooling rate of 3 K/min without any detailed dependences of the resistivity at various cooling rates.[25] From NMR, a sudden increase of T_1^{-1}, suggesting antiferromagnetic fluctuations, is not observed below 50 K; this resembles[26,27] the behavior of the isostructural salt θ-$(ET)_2CsZn(SCN)_4$ near 20 K. NMR studies on θ-RbZn in rapid cooling suggest that the charge density on the molecules becomes continuously distributed with decreasing temperature, as in the case of an incommensurate charge density wave (CDW). That may be described as a CO glasslike state when the charge density on every site becomes randomly distributed.

Diffuse scattering observed above T_{CO}—with $\boldsymbol{q}=(1/3,k,1/4)$—becomes weaker but still exists below T_{CO} in the rapid-cooled state (however, only at 4–5 K/min).[28] This indicates that the Q state has the nature of the room-temperature electronic state. But in the Q state below T_{CO} another diffuse rod of wave vector $\boldsymbol{q}_2=(0,k,1/2)$ was found to coexist. The modulation of $\boldsymbol{q}_2$ is also disordered in the interlayer direction (along b^*). After annealing at 180–190 K for around 12 h to get the R state, the diffuse rod $\boldsymbol{q}_2$ grows into a satellite reflection at $c^*/2$ resulting from the lattice dimerization.

We have previously shown[29] that the real part of the low-frequency dielectric permittivity, $\epsilon'(T)$, exhibits a sharp peak in the extreme vicinity of T_{CO}. We have also shown that ϵ' has a very small magnitude below T_{CO}, resulting from the lattice dimerization associated with the CO state. In the present paper, we report measurements of the conductivity and dielectric permittivity of θ-RbZn depending on the cooling rate. Bearing in mind the considerable difference in the relaxation times of the lattice and electron subsystems and using the various cooling rates as an instrument to distinguish between fast and slow processes involved in the phase transition in θ-RbZn, we will try to evaluate the relative contributions of these processes in the formation of the CO state in θ-RbZn.

II. EXPERIMENT

Electrical contacts were prepared using gold pads on the surface of the sample on which thin gold wires were attached afterward with silver paste. We carried out the measurements of the complex conductance $G(T,\omega)$ using an impedance analyzer (HP 4192A) in the frequency range 10^3-10^7 Hz and in the temperature range 4.2–295 K. The amplitude of the ac voltage field applied to the sample along the c axis was within the linear response regime and typically 30 mV/cm. Because the conductivity of this compound is relatively large (about 10 S/cm) we selected samples with minimum cross section (about 10^{-4} cm^2) and maximum length (several millimeters) in order to get samples with a maximum resistance most suitable for measurements using our impedance analyzer. The measurements of the complex conductance were carried out with an automatic setup under computer control. The resolution of our dielectric setup is estimated at about 5×10^3 at room temperature and 10^3 below T_{CO}.

We performed measurements with several coolings rates.

Slow cooling rate, typically 0.1–0.2 K/min, during which the temperature was stabilized at each point and measurements within the whole frequency range performed. The ground state thus reached below T_{CO} is the relaxed state (R state).

Fast cooling rate between 9 and 10 K/min. In this case, the temperature was not stabilized and data were taken at a unique frequency, namely, 1 MHz. The state at low temperature is the so-called quenched state (Q state).

Intermediate cooling rate, between 4 and 5 K/min, again without temperature stabilization and with measurements taken at frequency 1 MHz. We will call the state at low temperature reached in this condition the intermediate state (I state).

For the two last cooling rates, the temperature was read on the thermometer at the beginning of the data acquisition process, so there is a small difference in temperature of the sample between the beginning and the end of the data collection, which we estimate to be around 0.2 K.

In heating, we use the same processes: slow warming at 0.1 K/min and only intermediate heating with rate typically about 4 K/min.

III. RESULTS

A. Conductance

Figure 1 shows the temperature dependence of the real part of the conductance G of θ-RbZn, normalized by its value at room temperature, G_0, measured with cooling rates of 0.1, 4, and 9 K/min, while Fig. 2 shows the Arrhenius plot of the same data. In the temperature range 300–200 K the conductance decreases, i.e., it demonstrates a nonmetallic character of the conductivity. For the three cooling rates, in this temperature range, the $\log_{10} G(1/T)$ dependence is almost linear with, however, a slight upward curvature. If one ascribed this part of the $\log_{10} G(1/T)$ dependence to any

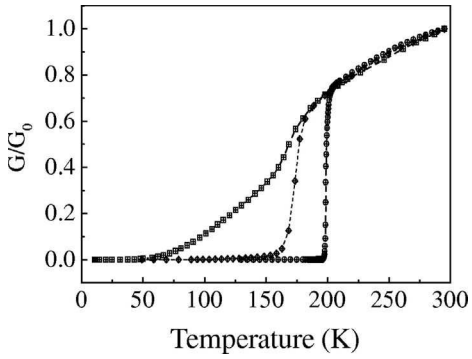

FIG. 1. Variation of the conductance G of θ-(BEDT-TTF)$_2$RbZn(SCN)$_4$ normalized by its room-temperature value G_0 as a function of temperature on cooling with three cooling rates: slow cooling at 0.1 K/min, relaxed state (○); intermediate cooling at 4 K/min, intermediate state (◇); and fast cooling at 9 K/min, quenched state (□).

thermoactivated process, then the appropriate energy gap would be 200 K, i.e., its magnitude would be close to the temperature of the measurements. Therefore, one cannot consider this variation of conductivity as a simple thermoactivated decrease of current carrier concentration due to the presence of some energy gap. Apparently, more complex processes occur in this temperature range; for example, temperature variation of the carrier scattering can occur, which will result in decrease of their mobility.

For slow cooling, below 200 K, the conductance decreases sharply by more than three orders of magnitude; after this jump the conductivity continues to decrease with a considerably larger energy gap $\Delta_{R\ \mathrm{state}} \approx 1900$ K. On heating, the phase transition occurs at a temperature 5 K higher than on cooling. These features are signatures of a first-order phase transition.

For fast cooling the conductance gradually decreases below 190 K without any sharp drop, indicating that the first-order character of the transition which occurs in slow cooling has been suppressed or at least greatly reduced. The logarithmic derivative of the conductance, however, exhibits a broad peak around $T=167$ K, which may indicate that some features of the phase transition occur at this temperature. The temperature dependence of the conductance at low temperature follows an activated behavior with an energy gap $\Delta_{Q\ \mathrm{state}} \approx 320$ K. Thus the conductivity at low T in the quenched state is much higher than in the relaxed state.

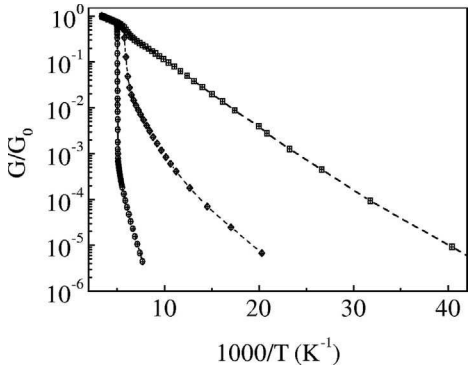

FIG. 2. Variation of the logarithm of the conductance G of θ-(BEDT-TTF)$_2$RbZn(SCN)$_4$ normalized by its room-temperature value G_0 as a function of inverse temperature on cooling with three cooling rates: slow (0.1 K/min), intermediate (4 K/min), and fast cooling (9 K/min).

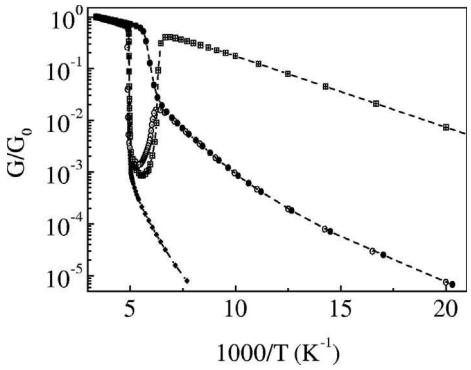

FIG. 3. Variation of the logarithm of the conductance G of θ-(BEDT-TTF)$_2$RbZn(SCN)$_4$ normalized by its room-temperature value G_0 as a function of inverse temperature measured on heating from the relaxed, intermediate, and quenched states obtained on cooling with different rates (Figs. 1 and 2). Heating rates: from the relaxed state, 0.1 K/min (◇); from intermediate (◎) and quenched states (□), 4–5 K/min. For comparison, data obtained with intermediate cooling are also shown (●).

The behavior for intermediate cooling is between those for slow and fast cooling: still a relatively sharp jump of the conductance with a peak in the logarithmic derivative at 168 K and an energy gap at low temperature $\Delta_{I\ \mathrm{state}} \approx 800$ K.

Figure 3 shows the temperature dependence of the conductance on heating from the R state, Q state, and I state. Let us compare first the T dependence of the conductance measured with intermediate cooling (already shown in Fig. 2) with that on heating at a rate of 4 K/min. From 50 to 160 K, there is no difference between cooling and heating, indicating that the I state is a metastable state. In the vicinity of 160 K, the conductivity decreases relatively sharply by more than one order of magnitude, goes through a minimum at about 180 K, and above this temperature joins the jumplike variation of the conductance of the relaxed state warmed at a slow heating rate of 0.1 K/min. A similar behavior occurs for the Q state: on heating, the conductance drops by three orders of magnitude at around 150 K and then joins the jumplike variation measured on heating from the R state. This means that, on heating, all the metastable states formed at low temperature from cooling rates with different amplitudes are destabilized, and that the stable ground state formed on slow cooling is recovered in the temperature range of 160–190 K. Thus, all the $G(1/T)$ curves show a first-order jump on heating near 200 K.

B. Dielectric permittivity

The temperature dependences of the real part of the dielectric permittivity $\epsilon'(T)$ at 1 MHz for several cooling rates

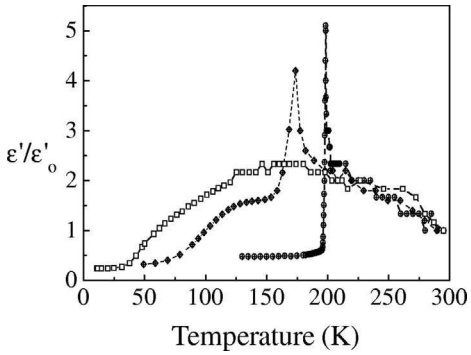

FIG. 4. Variation of the real part of the dielectric permittivity ϵ' of θ-(BEDT-TTF)$_2$RbZn(SCN)$_4$ normalized by its room-temperature value ϵ'_0 as a function of temperature on cooling with three cooling rates: slow cooling at 0.1 K/min, relaxed state (○); intermediate cooling at 4 K/min, intermediate state (◇); and fast cooling at 9 K/min, quenched state (□).

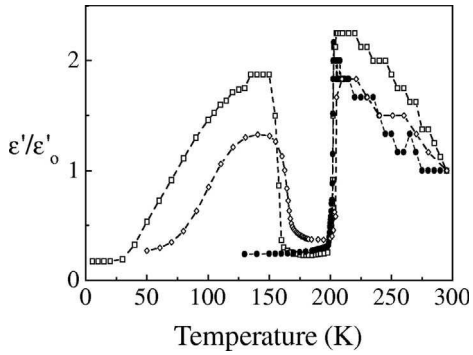

FIG. 5. Variation of the real part of the dielectric permittivity ϵ' of θ-(BEDT-TTF)$_2$RbZn(SCN)$_4$ normalized by its room-temperature value ϵ'_0 as a function of temperature on heating from the relaxed, intermediate, and quenched states obtained on cooling with different rates (Figs. 1 and 2). Heating rates: from the relaxed state, 0.1 K/min (○); from intermediate (◇) and quenched states (□), 4–5 K/min.

are shown in Fig. 4. We note that some parasite capacitance appears at room temperature after up and down temperature excursions have been performed. The origin of this effect could result from cracks and/or be due to some disorder from the quenched lattice distortion after annealing the Q or I state. Therefore, we present the dielectric constant dependences in a normalized form ϵ'/ϵ'_0, similar to G/G_0, ϵ'_0 being the dielectric permittivity at room temperature.

As was reported already earlier,[29] for slow cooling, $\epsilon'(T)$ shows a smooth monotonic growth beginning from room temperature. But near the temperature of the phase transition at T_{CO}, ϵ' exhibits a very sharp, close to divergent, growth in a very narrow temperature range. Just below T_{CO} a jumplike decrease of ϵ' occurs to a very small magnitude. On heating the jump of ϵ' is observed at a temperature about 5 K higher than on cooling.

As can be seen from Fig. 4, superposed on the background of the monotonic ϵ' growth, a peak of ϵ' appears in the extreme vicinity of T_{CO}, which resembles the $\epsilon'(T)$ peak measured at the CO transition in (TMTTF)$_2X$ salts,[30] thus indicating the possibility of ferroelectric character for the CO phase transition. The jump to a very low value of the dielectric permittivity ϵ' below T_{CO} is associated with the formation of the lattice superstructure and with the opening of the large energy gap $\Delta_{R\ \mathrm{state}}$. That means that the polarizability is strongly decreased by dimerization along the chains.

For intermediate cooling, the sharp increase of ϵ', a signature of the CO transition, occurs at a lower temperature, namely, 175 K. The temperature dependence from room temperature down to the CO transition is similar to that for slow cooling in this normalized plot. Below T_{CO} the dielectric constant decreases relatively fast down to 150 K (but much less than in the slow-cooling conditions) and shows below a broad shoulder before decreasing to a value beyond our resolution at low temperature.

For fast cooling there is no sign of any sharp divergence of ϵ'. The temperature dependence of ϵ' exhibits just a very broad maximum around 150–200 K. Again, between 200 K and room temperature, the $\epsilon'(T)$ dependence is similar for the three cooling rates.

On heating the relaxed state (obtained by slow cooling) the temperature dependence of the normalized ϵ' is shown in Fig. 5; as shown earlier,[29] ϵ' undergoes a very sharp jump at 205 K, 5 K higher than on cooling. From the Q state, on heating, ϵ' follows the same temperature dependence as on cooling up to about 160 K. Above this temperature the Q state is destabilized; ϵ' decreases to reach the value for slow cooling and then follows the same dependence as that measured in slow-cooling conditions. However, the magnitude of ϵ' reached above T_{CO} is about 50% larger than the value measured on slow cooling and, in addition, the $\epsilon'(T)$ dependence between T_{CO} and room temperature shows a curvature rather than a linear variation. A similar behavior occurs on heating the I state, except that the destabilization of the I state occurs at a slightly higher temperature, about 165 K.

Figure 6 shows in more detail a comparison of the temperature dependence of ϵ' on cooling and on heating for intermediate cooling. It appears that when, below T_{CO}, the metastable state is melted and the original CO state is restored, ϵ' drops to the value measured on slow cooling.

In the case of the I and Q states, ϵ' shows some frequency dispersion: at $T=130$ K ϵ' is nearly independent of fre-

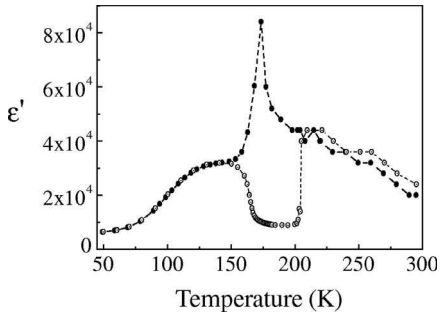

FIG. 6. Comparison of the temperature variation of the real part of the dielectric permittivity ϵ' of θ-(BEDT-TTF)$_2$RbZn(SCN)$_4$ on cooling at the rate 4 K/min (●) and on heating at the rate 4–5 K/min (◎).

quency up to 6×10^5 Hz but decreases at higher frequencies nearly as a power law, ϵ' changing from 8×10^4 at 0.6 MHz to 5×10^4 at 3 MHz.

IV. DISCUSSION

As shown above, the phase transition into the CO state is strongly dependent on the cooling rate as well as the magnitude of the effective energy gap below T_{CO}: $T_{CO}=200$ K at the slow cooling (0.1 K/min) and 168 K at the intermediate cooling rate (4–5 K/min). In fast cooling (9–10 K/min), a small bump is observed on the $G(1/T)$ curve (minimum of the logarithmic derivative at 167 K) with a subsequent small variation of its slope below this temperature. This means that the quenched state is not fully equivalent to the initial state at $T>T_{CO}$, i.e., probably even at such a fast cooling rate, θ-RbZn has time for a partial relaxation.

For any cooling rate, the low-temperature state below 150 K is fairly well stable at least for several hours. The possibility of relaxation of the Q state and also the I state appears only when the temperature is increased above 160 K. The whole hysteresis of conductance between cooling and heating cycles, which corresponds to three orders of magnitude of G (Fig. 3), is observed only in the temperature range 160–200 K.

As can be seen from Fig. 4, and as was shown earlier,[29] on slow cooling, the divergency of ϵ' near T_{CO} is associated with the formation of the three-dimensional CO state with a reasonably large correlation length. At the intermediate cooling rate, the peak of $\epsilon'(T)$ still exists although its magnitude is smaller and its width larger than on slow cooling. Additionally, the $\epsilon'(T)$ peak is observed at a lower temperature: 175 K (Fig. 4). Accordingly, the intermediate state can be characterized as a CO state but with a smaller correlation length. Finally, at a cooling rate about 10 K/min, the peak in the $\epsilon'(T)$ dependence is not observed at all, i.e., at such a cooling rate, only a short-range CO state can be realized, which is probably similar to a glassy CO state.[25]

Figure 4 shows that, in the temperature range above T_{CO}, the $\epsilon'(T)$ dependences coincide qualitatively for various cooling rates. The state formed in this temperature range is weakly associated with lattice deformations. The low-temperature (5–160 K) short-range CO state, obtained at intermediate and fast cooling rates, is characterized by the same $\epsilon'(T)$ dependences on cooling and heating cycles (Fig. 1), i.e., the short-range CO state is fairly stable in this temperature range. All relaxation processes are accelerated in the temperature range 160–200 K where the maximum difference in the ϵ' magnitude is observed depending on the cooling rate (Fig. 6). On heating, the abrupt increase of ϵ' occurs at practically the same temperature. As was noted above, the dependences of conductance $G(T)$ also show analogous behavior.

Nonlinear current-voltage characteristics have been measured in the insulating states of θ-$(ET)_2RbZn(SCN)_4$ (Ref. 31) and θ-$(ET)_2CsZn(SCN)_4$,[32] and attributed to collective excitations associated with charge ordering. In θ-$(ET)_2CsZn(SCN)_4$, the large nonlinear conductivity is just like that of a sliding CDW although there are no signs of CO long-range order. This latter behavior is reminiscent of recent measurements on manganites; the superstructure, previously attributed to charge localization, was considered to resemble a charge density wave[33] with collective transport properties,[34] although no clear feature of any CDW ordering temperature was observed.

We can suggest the following explanation of these results. As is known, the phase transition into the CO state in θ-RbZn salt which is driven by electron-electron correlations,[15,16] is accompanied by an essential lattice transformation with doubling of its period along the c axis. In this respect, a question arises about the possibility of realization of a long-range CO state without any appropriate lattice transformation. The results mentioned above show that, at fairly large cooling rates, when the ordered lattice superstructure at $c^*/2$ has not enough time to develop over a considerably large distance—only diffuse rods are detected[28]—the divergence of ϵ' is not observed. That means that, in the θ-RbZn salt, the sole effect of electron-electron correlations is probably not sufficient for the formation of the long-range CO state. For stabilization of this state it seems that the appropriate lattice transformation is needed.

As was noted[30] in quasi-one-dimensional compounds of the $(TMTTF)_2X$ family, where electron-phonon interactions are relatively weak, the factor stabilizing the CO state is, most likely, a shift as a whole of the fairly mobile sublattice of anions (transition at $q=0$). Apparently, in quasi-two-dimensional compounds, the mobility of the anion sublattice is smaller; but electron-phonon interactions at $T<T_{CO}$ become fairly strong, which provides stabilization of the CO state by formation of a superlattice with $c^*/2$. This cooperative action can minimize the free energy of the system by lowering the electronic and structural symmetry.[8,16] In developing these ideas, the question can be raised about overcoming the geometrical frustration which can develop at the transition into the CO state in the triangular lattice structure characteristic for the θ-RbZn salt.[16,35] On a triangular lattice, charges are frustrated against a periodic ordering; this follows the mean-field study of the extended Hubbard model, suggesting that several types of periodic CO are degenerate. In this respect, the combined CO and structural transition can be considered as an "attempt" of the compound to relax the frustration by lowering the lattice symmetry.[16]

However, the relaxation times characteristic of electron systems are usually considerably faster than those for lattices, especially in the case of molecular crystals consisting of large molecules. As a result, the lattice does not have enough time to transform in the appropriate manner at fairly fast cooling rates through the temperature range of the CO transition. The form of the state developed will be dependent on the cooling rate. A fast cooling leads probably to the formation in θ-RbZn of a disordered short-range superstructure with different degrees of lattice transformation toward the $c^*/2$ superstructure. At the intermediate cooling rate (4–5 K/min), θ-RbZn probably has enough time for transformation into a state characterized by some intermediate CO order. Correspondingly, some features of the phase transition on slow cooling in $G(1/T)$ and $\epsilon'(T)$ curves are preserved, with some intermediate values for the critical tem-

perature and the energy gap (Figs. 2 and 4). At the fastest cooling (about 10 K/min) the greater part of the sample stays in the metastable state characteristic of the temperature range $T > T_{CO}$. The results for x-ray spectroscopy,[7] NMR,[17,18,27] and magnetic susceptibility[24] in θ-RbZn, mentioned in the Introduction, lead to the same conclusions. For example, the broadened spectral features can be a sign of glassy disproportionation, which is the charge equivalence of the spin glass. All of that shows that the Q state is a rather disordered short-range CO state, which, however, can relax to some appropriate equilibrium (more homogeneous) long-range CO state as a result of annealing. The experimental data obtained by us are in good agreement with the qualitative picture presented here of the formation of CO states in quasi-two-dimensional organic compounds.

V. CONCLUSION

The results presented show an essential modification of the temperature dependences of the conductance and the real part of the dielectric permittivity in θ-$(ET)_2RbZn(SCN)_4$ on the cooling rate. With increasing cooling rate, the sharpness of the first-order phase transition into the charge-ordered state decreases considerably, and features of the developed low-temperature state are determined by this cooling rate. These results favor the important role of electron-phonon interactions and of the combined character (electron and lattice contributions) of the transition into the charge-ordered state in these quasi-two-dimensional organic compounds.

ACKNOWLEDGMENTS

We are grateful to T. Nakamura for sending us his results on magnetic susceptibility at different cooling rates before publication. This work was supported in part by the Russian Foundation for Basic Research (Grant No. 06-02-72551) in the frame of the CNRS-RAS Associated European Laboratory of the Institute Néel and the Institute of Radioengineering and Electronics RAS, and partially by INTAS (Grant No. 05-1000008-7972).

[1] For a recent review, see H. Fukuyama, J. Phys. Soc. Jpn. **75**, 051001 (2006).
[2] J. M. Tranquada, B. J. Sternlieb, J. D. Axe, Y. Nakamura, and S. Uchida, Nature (London) **375**, 561 (1995).
[3] S. Mori, C. H. Mori, and S. W. Cheong, Nature (London) **392**, 473 (1998).
[4] H. Kino and H. Fukuyama, J. Phys. Soc. Jpn. **65**, 2158 (1996).
[5] H. Mori, I. Hirabayashi, S. Tanaka, T. Mori, and Y. Maruyama, Synth. Met. **70**, 789 (1995).
[6] H. Mori, S. Tanaka, and T. Mori, Phys. Rev. B **57**, 12023 (1998).
[7] M. Watanabe, Y. Noda, Y. Nogami, and H. Mori, J. Phys. Soc. Jpn. **73**, 116 (2004).
[8] K. Miyagawa, A. Kawamoto, and K. Kanoda, Phys. Rev. B **62**, R7679 (2000).
[9] R. Chiba, H. M. Yamamoto, K. Hiraki, T. Nakamura, and T. Takahashi, Synth. Met. **120**, 919 (2001).
[10] R. Chiba, H. M. Yamamoto, K. Hiraki, T. Takahashi, and T. Nakamura, J. Phys. Chem. Solids **62**, 389 (2001).
[11] K. Yamamoto, K. Yakushi, K. Miyagawa, K. Kanoda, and A. Kawamoto, Phys. Rev. B **65**, 085110 (2002).
[12] T. Takahashi, R. Chiba, K. Hiraki, H. M. Yamamoto, and T. Nakamura, J. Phys. IV **114**, 269 (2004).
[13] R. Chiba, K. Hiraki, T. Takahashi, Y. M. Yamamoto, and T. Nakamura, Synth. Met. **133-134**, 305 (2003).
[14] R. Chiba, K. Hiraki, T. Takahashi, H. M. Yamamoto, and T. Nakamura, Phys. Rev. Lett. **93**, 216405 (2004).
[15] H. Seo, J. Phys. Soc. Jpn. **69**, 805 (2000).
[16] H. Seo, C. Hotta, and H. Fukuyama, Chem. Rev. (Washington, D.C.) **104**, 5005 (2004).
[17] R. Wojciechowski, K. Yamamoto, K. Yakushi, M. Inokuchi, and A. Kawamoto, Phys. Rev. B **67**, 224105 (2003).
[18] H. Tajima, S. Kyoden, H. Mori, and S. Tanaka, Phys. Rev. B **62**, 9378 (2000).
[19] H. Mori, T. Okano, S. Tanaka, M. Tamura, Y. Nishio, K. Kajita, and T. Mori, J. Phys. Soc. Jpn. **60**, 1751 (2000).
[20] H. Fukuyama and H. Seo, J. Phys. Soc. Jpn. **66**, 1249 (1997).
[21] T. Nakamura, R. Kinami, W. Minagawa, T. Takahashi, H. Mori, S. Tanaka, and T. Mori, Mol. Cryst. Liq. Cryst. Sci. Technol., Sect. A **285**, 1991 (1996).
[22] T. Nakamura, W. Minagawa, R. Kinami, Y. Konishi, and T. Takahashi, Synth. Met. **103**, 1898 (1999).
[23] T. Nakamura, W. Minagawa, R. Kinami, Y. Konishi, and T. Takahashi, Mol. Cryst. Liq. Cryst. Sci. Technol., Sect. A **285**, 57 (1996).
[24] T. Nakamura (private communication).
[25] K. Kanoda, K. Ohnou, M. Kodama, K. Miyagawa, and T. Itou, J. Phys. IV **131**, 21 (2005).
[26] T. Nakamura, W. Minagawa, R. Kinami, and T. Takahashi, J. Phys. Soc. Jpn. **69**, 504 (2000).
[27] K. Suzuki, K. Yamamoto, K. Yakushi, and A. Kawamoto, J. Phys. Soc. Jpn. **74**, 2631 (2005).
[28] M. Watanabe, Y. Noda, Y. Nogami, and H. Mori, Synth. Met. **135-136**, 665 (2003).
[29] F. Nad, P. Monceau, and H. M. Yamamoto, J. Phys.: Condens. Matter **18**, 2509 (2006).
[30] For a review, see F. Nad and P. Monceau, J. Phys. Soc. Jpn. **75**, 051005 (2006).
[31] Y. Takahide, T. Konoike, K. Enomoto, M. Nishimura, T. Terashima, S. Uji, and H. M. Yamamoto, Phys. Rev. Lett. **96**, 136602 (2006).
[32] K. Inagaki, I. Terasaki, H. Mori, and T. Mori, J. Phys. Soc. Jpn. **73**, 3364 (2004).
[33] S. Cox, J. C. Lashey, E. Rosten, J. Singleton, A. J. Williams, and P. B. Littlewood, J. Phys.: Condens. Matter **19**, 192201 (2007).
[34] S. Cox, J. Singleton, R. D. McDonald, A. Migliori, and P. B. Littlewood, arXiv:0705.4310v1.
[35] J. Merino, H. Seo, and M. Ogata, Phys. Rev. B **71**, 125111 (2005).